CAR T cells targeting BAFF-R can overcome CD19 antigen loss in B cell malignancies

Authors: Hong Qin[1]†, Zhenyuan Dong[1]†, Xiuli Wang[2], Wesley A. Cheng[1], Feng Wen[1,3], Weili Xue[1,4], Han Sun[1], Miriam Walter[2], Guowei Wei[1], D. Lynne Smith[1], Xiuhua Sun[5], Fan Fei[6], Jianming Xie[6], Theano I. Panagopoulou[7], Chun-Wei Chen[7], Joo Y. Song[8], Ibrahim Aldoss[9], Clarisse Kayembe[10], Luisa Sarno[10], Markus Müschen[7], Giorgio G. Inghirami[10], Stephen J. Forman[2], Larry W. Kwak[1]*.

Affiliations:

[1]Toni Stephenson Lymphoma Center, Department of Hematology and Hematopoietic Cell Transplantation, Beckman Research Institute of City of Hope, Duarte, California, 91010, USA.

[2]Center for CAR T Cell Therapy, Department of Hematology and Hematopoietic Cell Transplantation, Beckman Research Institute of City of Hope, Duarte, California, 91010, USA.

[3]Department of Medical Oncology Cancer Center, West China Hospital, Sichuan University, Sichuan, 910041, China.

[4]The First Affiliated Hospital of Zhengzhou University, Zhengzhou, 450001, China.

[5]The Second Affiliated Hospital of Dalian Medical University, Dalian, 116044, China.

[6]Department of Pharmacology and Pharmaceutical Sciences, School of Pharmacy, University of Sothern California, California, 90007, USA.

[7]Department of Systems Biology, Beckman Research Institute of City of Hope, Duarte, California, 91010 USA.

[8]Department of Pathology, City of Hope National Medical Center, Duarte, California, 91010, USA.

[9]Gehr Family Center for Leukemia Research, Department of Hematology and Hematopoietic Cell Transplantation, Beckman Research Institute of City of Hope, Duarte, California, 91010, USA.

[10]Department of Pathology and Laboratory Medicine, Weill Cornell Medical College, New York, New York, 10065, USA

†These authors contributed equally.

*Corresponding author:

Larry W. Kwak, MD, PhD
lkwak@coh.org

OVERLINE: CANCER

One Sentence Summary: BAFF receptor is a target for CAR T cell therapy of B cell malignancies, circumventing issues with CD19 antigen loss in tumors.

Abstract:

CAR T cells targeting CD19 provide promising options for treatment of B cell malignancies. However, tumor relapse from antigen loss can limit efficacy. We developed humanized, second-generation CAR T cells against another B cell specific marker, B cell activating factor-receptor (BAFF-R), which demonstrated cytotoxicity against human lymphoma and acute lymphocytic leukemia (ALL) lines. Adoptively transferred BAFF-R-CAR T cells eradicated 10-day pre-established tumor xenografts after a single treatment, and retained efficacy against xenografts deficient in CD19 expression, including CD19-negative variants within a background of CD19-positive lymphoma cells. Four relapsed, primary ALLs with CD19 antigen loss obtained after CD19-directed therapy retained BAFF-R expression and activated BAFF-R-, but not CD19-CAR T cells. BAFF-R-, but not CD19-CAR T cells, also demonstrated antitumor effects against an additional CD19 antigen loss primary patient-derived xenograft (PDX) *in vivo*. BAFF-R is amenable to CAR T-cell therapy and its targeting may prevent emergence of CD19 antigen loss variants.

Introduction:

Chimeric antigen receptor (CAR) T cells directed against CD19 have shown excellent response rates for treatment of lymphomas and leukemia (*1-5*). Despite high initial efficacy, some patients relapse through different modes of disease recurrence. One mode is CD19-negative relapse with CD19 surface expression loss, likely resulting from consequent mutations and selection for alternatively spliced isoforms. Another involves CD19-positive relapse with CD19 surface expression retained, likely resulting from rapid disappearance or decreased function of the CAR T cells (*6, 7*). An estimated 20-30% of relapses post CD19-CAR T-cell therapy involve antigen loss, pointing to the urgent need to identify alternative targets and improve efficacy and persistence of CAR T cells (*6*). We developed humanized, second-generation CAR T cells against another B-cell specific marker, B-cell activating factor-receptor (BAFF-R), a target for immune therapy of cancer that has not been fully realized. BAFF-R is a B-lineage marker with expression restricted to B cells after the progenitor stage and before the plasma cell stage of development, including malignant B cell counterparts. Its function has been well characterized, and studies show that its expression is critically required for normal B cell survival (*8-12*). These characteristics may thus limit the ability of malignant B cells to evade BAFF-R-directed therapies by downregulation. We test BAFF-R-directed CAR T cells against human lymphoma and acute lymphocytic leukemia (lines) in vitro and in mouse models in comparison to CD19-directed CAR T cells. Specifically, we test BAFF-R CAR T cell activity against CD19-negative targets.

Results

Generation and Characterization of BAFF-R-CAR T cells.

A humanized, single-chain variable fragment (scFv) derivative of a mouse anti-human BAFF-R antibody (*13*) was engineered onto a second generation CAR construct containing 4-1BB costimulatory and CD3ζ intracellular signaling domains. Healthy donor T-cell subpopulations were selected, transduced by BAFF-

R CAR, enriched, expanded, and tested for specific activation by BAFF-R expressing targets (**Fig. 1A**). Considerable amounts of TNF-α, IFN-γ, and granzyme B were released by CD4 and CD8 CAR T cells co-incubated with human BAFF-R expressing mouse fibroblast L cells (B2D) and human mantle cell lymphoma (MCL) lines (JeKo-1 and Z-138), compared with BAFF-R-negative parental (L) cells. Allogeneic reactions were excluded by including corresponding non-transduced T cells from the same donors (non-CAR, **fig. S1**). CD8-, and to a lesser extent CD4-, derived BAFF-R-CAR T cells also elicited specific cytotoxicity against a panel of human lymphoma cell lines and leukemia cell lines (**Fig. 1B, fig. S2**). In addition, CD8-, and to a lesser extent CD4-, derived BAFF-R-CAR T cells elicited significant specific cytotoxicity against multiple primary human lymphoma subtypes ($P<0.0001$ vs. controls, **Fig. 1C**).

BAFF-R-CAR T- cell subpopulations demonstrated robust in vivo antitumor effects

Next, we tested CAR-transduced human T-cells for therapeutic efficacy against 10-day pre-established human Raji Burkitt lymphoma xenografts in immunocompromised mice. Because T cell phenotypes can affect CAR T cell function, we tested different mixtures of T cells (*14-19*). Remarkable tumor regression and prolonged survival were observed after treatment with CAR-transduced Pan-T cells (**Fig. S3**) or defined mixtures of CD4 naïve T cells (T_N) with either T_N, central memory (T_{CM}), or stem memory (T_{SCM}) enriched CD8 CAR T cells, compared with either non-transfected T cells or PBS controls (**Fig. 2A, Fig. S3**). Furthermore, at the minimum therapeutic dose of $2x10^6$ cell (1:1 ratio of CD4:CD8 CAR T cells) we observed superior therapeutic effects mediated by CD8 T_N CAR T cells, as demonstrated by 80% long-term survival compared with 20% and 40% survival, respectively by CD8 T_{CM} and T_{SCM} CAR T cells (**Fig. 2B**).

We also tested the therapeutic efficacy of T_N-derived BAFF-R-CAR T cells against an aggressive CD19-positive Burkitt lymphoma (Raji) line (**Fig. 3A, Fig. S4**). Mice with previously established tumors were

treated with a single dose of defined mixtures of T_N CD4 and CD8 BAFF-R- or CD19-CAR T cells (*20*) (identical CAR backbone) on day 7. Compared with control mice treated with non-CAR T cells or PBS, mice treated with CD19-CAR T cells exhibited delayed, but progressive lethal tumor growth. In contrast, mice treated with BAFF-R-CAR achieved complete tumor regression, with 100% long-term survival (**Fig. 3B**). As one potential explanation of the difference between BAFF-R- and CD19-CAR T cell efficacy, we characterized respective surface antigen density on Raji and several other lymphoma and leukemia lines. Surprisingly, BAFF-R surface antigen density was significantly lower than that of CD19 on all cell lines ($P<0.0001$ BAFF-R vs. CD19, **Fig. 3C**).

Therapeutic effects of BAFF-R CARs against human CD19-negative B-cell tumor lines in vitro and in vivo. One strategy to overcome the problem of antigen-loss tumor escape variants emerging after successful CD19-targeted therapies is to target alternative cell surface molecules, such as BAFF-R. We modeled disease relapse due to the loss of CD19 by generating CRISPR CD19 gene knock-out of multiple human B-cell tumor lines, including MCL (Z-138), CLL (MEC-1), and ALL (Nalm-6) and a gRNA-silenced CD19 gene knock-down of an ALL PDX (*21-23*) (**Fig. 4A-B, Fig. S5**). CD19 expression on all resulting cell lines was absent by surface staining, whereas BAFF-R expression was not affected, as expected. We then tested CD8 T_N-derived BAFF-R- or CD19-CAR T cells for cytotoxicity against both wild-type and CD19-negative tumor cells in vitro. CD19-CAR T cells demonstrated cytotoxicity only against wild-type tumor cells, whereas BAFF-R-CAR T cells maintained cytotoxicity against both wild-type and CD19-negative tumors.

The therapeutic efficacy of BAFF-R-CAR T cells was tested against human MCL Z-138-CD19-deficient xenografts established in NOD *scid* gamma (NSG) mice (**Fig. 4C**). A single dose of a defined mixture of T_N CD4 and CD8 BAFF-R-CAR T cells infused on day 11 completely eliminated established tumors. In contrast, treatment with identical mixtures of CD19-CAR T cells or non-transduced T cells from the same

donor or PBS was associated with progressive tumor growth. Similar results were also observed against ALL Nalm-6-CD19KO xenografts *in vivo* (**Fig. 4D**).

We next challenged NSG mice with Z-138 CD19-deficient cells spiked into a background of wild type Z-138 cells to determine whether CAR T cells could prevent the emergence of a pre-existing CD19-negative tumor population. NSG mice were challenged with a mixture of 5 x 10^4 Z-138 (wildtype,CD19-positive) plus 5 x 10^4 Z-138-CD19 deficient tumor cells, and then groups of 5 tumor-bearing mice each were randomly assigned to a single treatment with either 2.5 x 10^6 CD4 T_N + 10^6 CD8 T_N BAFF-R- or CD19-CAR T cells per mouse on day 8 (**Fig. 5A-B**). Non-transduced T cells from the same donor were used as allogeneic controls (non-CAR). As shown, only BAFF-R CAR T cells were able to eradicate both tumor populations, whereas CD19 CAR T cell treatment was associated with emergence of CD19-deficient tumor and treatment failure (**Fig. 5C**).

BAFF-R-specific CAR T-cell activation by CD19 antigen loss primary human tumors

Finally, we tested BAFF-R-CAR T cells against a panel of cryopreserved primary CD19-negative tumor samples, obtained from four patients at the time of relapse after CD19-targeted therapy (CD19/CD3 bi-specific T-cell engager antibody, BiTE, blinatumomab (*24*)). Cell surface staining demonstrated CD19 and BAFF-R expression by corresponding tumors obtained prior to CD19-targeted therapy. However, post-treatment samples exhibited clear down-regulation of CD19, while retaining positive BAFF-R expression (**Fig. 6A**). Following depletion of patient T cells from tumor samples, specific effector function of either CD19- or BAFF-R-CAR T cells against paired pre- and post-CD19 BiTE therapy primary tumor cells was first determined by expression of degranulation marker CD107a on CAR T cells. Activation of CD19-CAR T cells by all four CD19-negative post therapy tumors was substantially reduced, compared with BAFF-R-

CAR T cells and with corresponding available CD19-positive pre-therapy tumors, whereas BAFF-R-CAR T cells were equally activated by pre- and post-CD19-targeted therapy tumors (**Fig. 6B**).

A fifth B-ALL patient sample obtained at relapse was used for *in vivo* PDX engraftment. These B-ALL blasts were CD19-negative and BAFF-R-positive (**Fig. 6C**). B-ALL blasts were successfully engrafted, and by 26 days peripheral blasts reached 1-5% of total cells (human/mouse, **Fig. 6D**). Mice were randomly assigned to treatment with BAFF-R-or CD19-CAR T cells (5 x 10^6, 1:1 CD4:CD8 T_N ratio/mouse) on day 26. Non-transduced CD4/CD8 T cells from the same donor were used as allogeneic controls (non-CAR). Analysis on day 54 revealed significantly fewer circulating tumor cells in BAFF-R CAR T-cell treated mice, compared with CD19 CAR T-cell or control treated mice ($P<0.0001$). BAFF-R CAR T-cell treated mice also demonstrated significantly prolonged survival compared to all other groups ($P<0.01$, **Fig. 6E**).

Discussion

BAFF-R is a highly expressed B-cell lineage surface marker by various B-cell malignancies, making it an appealing target for immunotherapy. Mechanistically, BAFF-R-signaling activates NF-κB pathways to promote tumor survival and proliferation (*25, 26*) and increased BAFF-R expression correlated with disease progression in patients with B-cell lymphoma and pre-B ALL (*27-29*). Furthermore, mouse strains expressing a mutant BAFF-R exhibit decreased B-cell life spans (*30*), associated with a substantially reduced peripheral B-cell compartment, and BAFF-R-null mice exhibit greatly reduced B-cell numbers and are essentially devoid of marginal zone B cells (*8, 31*). Collectively, these reports suggest that BAFF-R signaling is a driver of B-cell growth and survival. This critical feature may also limit the capacity of B-cell tumors to escape therapy by down-regulation of BAFF-R expression (*10, 32-34*).

The BAFF/BAFF-R axis has been targeted successfully for autoimmune diseases, particularly with mAbs against the BAFF ligand (*35, 36*); however, the promise for cancer therapy has not yet been realized. Most previously described mAbs against the receptor (*37*) failed to demonstrate efficacy against human B-cell tumors (*11, 12*). More recently, targeting BAFF-R with mAbs showed efficacy against CLL in preclinical models, particularly when combined with a Bruton tyrosine kinase inhibitor (*38*), and this mAb has entered clinical trials (NCT03400176). A preliminary report targeting BAFF-R using a CAR platform was limited to *in vitro* studies of ALL (*39*).

Although CD19-CAR T-cell therapy is effective in many patients with B-ALL or lymphoma, CD19-negative tumor cells are observed in 30% of post CD19-directed BiTE or CAR T-cell therapy relapses, underscoring the urgent need to exploit alternative targets (*6, 40*). CAR T cells targeting the B-lineage marker CD22 have been proposed as one alternative strategy to overcome relapse from CD19 antigen loss, as demonstrated by achievement of durable clinical responses in patients with CD19-negative B-ALL (*41-43*). Importantly, this clinical trial also demonstrated comparable potency of CD22-CAR T cells to that of CD19-CAR T cells at biologically active doses. However, relapses were associated with diminished CD22 site density that likely permitted CD22-negative cells to escape killing by CD22-CAR T cells.

We modeled CD19 antigen loss by CD19 gene knockout of multiple B-ALL and lymphoma cell lines and observed retention of susceptibility to cytotoxicity *in vitro*, and tumor eradication *in vivo* by BAFF-R-, but not CD19-CAR T cells. These *in vitro* findings were also verified in a primary PDX ALL tumor in which knockdown of CD19 expression had been achieved. We further modeled one mechanism of CD19-negative escape by demonstrating that BAFF-R-, but not CD19-CAR T cells, could prevent the emergence of CD19-deficient tumor cells when spiked into a background of wild type tumor *in vivo*. Finally, using four primary CD19-negative ALL tumor escape variants emerging naturally from patients treated with

prior CD19-directed therapies, we demonstrated retention of BAFF-R expression, specific activation of BAFF-R-, but not CD19-CAR T cells *in vitro*, and antitumor effects and prolonged survival specifically associated with BAFF-R CAR T-cell treatment against one additional primary PDX *in vivo*. Together, the findings suggest the potential effectiveness of BAFF-R-CAR T cells in the setting of CD19 antigen loss. Under the specific experimental conditions selected, the therapeutic effects of our BAFF-R-CAR T cells exceeded that of CD19-CAR T cells produced using the same second generation CAR backbone and administered at identical doses, particularly *in vivo*. The specific reasons for this therapeutic discrepancy between BAFF-R- and CD19-CAR T cells remain to be elucidated by additional investigation.

To our knowledge, given that there is no existing model of spontaneous CD19-negative antigen loss due to immunologic pressure of CD19-targeted therapy against human tumor xenografts in immunocompromised mice, the use of BAFF-R-CAR T cells to demonstrate true rescue of tumor escape variants must await the development of suitable models. Another potential limitation of our study is that although the critical role of BAFF-R signaling on normal B cell survival strongly suggests that antigen loss emerging from BAFF-R targeting is not likely, the definitive test of this potential mechanism of resistance to BAFF-R-CAR T cell therapy must await human trials, which are planned. As with most preclinical CAR T cell studies, recipient mice were immunodeficient, so side effects in an intact immune environment would not be detected.

Taken together, our data suggest that further development of BAFF-R-directed adoptive T-cell therapies is warranted for B-cell malignancies. Future strategies combining dual targeting of CD19 and BAFF-R may also be warranted.

Materials and Methods:

Study design

The overall objective of this study was to demonstrate that BAFF-R is a suitable target for CAR T-cell therapy against CD19 antigen loss disease. A novel BAFF-R CAR T cell was developed to test this hypothesis in vitro and in vivo. The in vitro experiments consisted of cell surface staining characterization of both target and CAR T cells and functional cytotoxic T lymphocyte, chromium release assays. All in vitro assays were performed with at least triplicate samples. Due to the limited availability of primary patient samples, replicate testing was not always possible. In vivo studies were performed with n=5 mice per group of 8-12 week old mice. Experiments were repeated at least 3 times. Based on the previous studies to establish the tumor models, the survival data in two-sided log-rank tests have least 80% power at an overall 0.05 significance level to detect a hazard ratio (HR) of 0.15. Tumor challenged mice were randomized into treatment groups. Treatments were not administered blinded, however mice were monitored for signs of distress and humane endpoints in a blinded manner. Veterinary staff, independent of the researchers and studies, monitored mice daily and alerted researcher when a humane endpoint had been reached. All studies were performed under approved Institutional Animal Care and Use Committees (IACUC) and Institutional Review Board (IRB) protocols. Primary data are reported in data file S1.

Animals

NSG mouse breeding pairs were purchased from The Jackson Laboratory (Stock No.: 005557). The NSG breeding colony was maintained by the Animal Resource Center at City of Hope. Mice were housed in a pathogen-free animal facility according to institutional guidelines. All animal studies were approved by the Institutional Animal Care and Use Committee (IACUC: 15020). NSG mice used in the in vivo PDX model

were bred within the Sandra and Edward Meyer Cancer Center PDTX Animal Core, under strict specific and opportunistic pathogen free (SOPF) conditions (protocol number 2014-0024).

Cell lines

Malignant human hematologic cell lines including JeKo-1, Raji, OCI-LY10, RL, RS4;11, MEC-1, Nalm-6 were purchased from either ATCC or DSMZ. Mouse fibroblast L cells, HT1080 human epithelial cells, and 293FT cells were obtained from ATCC. Z-138 cell line was provided by Dr. Michael Wang (MD Anderson Cancer Center). Banks of all cell lines were authenticated for the desired antigen/marker expression by flow cytometry prior to cryopreservation, and thawed cells were cultured for less than 6 months prior to use in assays.

Human blood and primary tumor samples

Non-cultured, primary human lymphomas were obtained as cryopreserved, viable single cell suspensions in 10% DMSO from the Lymphoma Satellite Tissue Bank at MD Anderson Cancer Center under an Institutional Review Board approved protocol (IRB: 2005-0656). Primary patient samples included PBMC from leukapheresis or blood from patients with mantle cell lymphoma (MCL), and excised lymph nodes from patients with diffuse large B-cell lymphoma (DLBCL) or follicular lymphoma (FL). Tumor cells in each sample ranged from 80% to 98% for leukapheresis or blood, and from 50% to 60% for lymph node biopsies. Primary human ALL samples were obtained from the Pathology: Liquid Tumor Core tissue bank at City of Hope (IRB: 03162). Peripheral blood mononuclear cells (PBMC) from healthy donors were provided by the Michael Amini Transfusion Medicine Center at City of Hope (IRB: 15283).

CAR T-cell production

A second generation BAFF-R CAR was generated consisting of the humanized H90 BAFF-R antibody scFv(*13*), CD8 transmembrane, 4-1BB and CD3ζ intracellular signaling domains. The CAR cDNA was cloned into pLenti7.3 lentiviral vector (pLenti7.3/V5-DEST Gateway Vector Kit, Invitrogen). CD19 CAR was generated in the same way, replacing BAFF-R antibody scFv with CD19 antibody scFv.(*20*) Lentiviruses were produced in 293FT cells, concentrated and titered with HT1080 human epithelial cells.

CD4 and CD8 naïve T cells (T_N) from the same healthy donor were isolated with Human Naïve CD4+ or CD8+ T Cell Isolation Kits, respectively (Stemcell Technologies). To isolate CD8 central memory T cells (T_{CM}), CD8 T cells prepared with EasySep Human CD8+ T Cell Enrichment Kit (Stemcell Technologies) were stained with CD8-PerCP-Cy5.5, CD45 RO-APC and CD62L-PE and sorted for CD8+/CD45RO+/CD62L+ stem memory T cells (T_{SCM}) CD8 T_{SCM}-like cells were generated by CD8 T_N cultured in AIM-V medium supplemented with 5% human serum, 5 ng/mL IL-7, and 30 ng/mL IL-21. 5 mM TWS119 (GSK3 inhibitor) was supplemented to inhibit differentiation and retain the T_{SCM}-like state. All T cells were activated with Human T-Activator CD3/CD28 beads (Life Technologies) for 24 h followed by transduction with lentivirus encoding CAR/GFP at MOI=1. Following 7 d in culture, GFP-positive CAR-T cells were enriched by FACS and further activated and expanded with CD3/CD28 bead stimulation for another 7 d. Only productions that yielded ≥95% GFP-positive CAR-T cells were used for further studies.

Cytokine production assay

CAR-T cells were co-incubated for 24 h with BAFF-R expressing target cells (tumor lines) at an effector-to-target (E:T) ratio of 2:1. Controls included BAFF-R-negative L cells, BAFF-R-positive B2D cells, CD3/CD28 beads (10 µL/10^6 CAR-T cells), and non-transduced T cells from the same donor. Supernatant was collected for ELISA detection of cytokines (Human IFN-γ ELISA Set and Human TNF ELISA Set, BD Biosciences) and granule release (Human Granzyme B DuoSet ELISA Kit, R&D).

Cytotoxic T lymphocyte (CTL) assay

A standard chromium-51 (^{51}Cr) release assay was used to calculate specific lysis by CAR-T cells. Briefly, target cells (tumor cell lines or primary patient tumors) were radiolabeled with ^{51}Cr (PerkinElmer). CAR-T cells were co-incubated with labeled target cells at E:T ratios ranging from 1:1 to 10:1 for 4 h. Controls included non-transduced T cells from the same donor. Clarified supernatant was sampled for ^{51}Cr detection in a Wizard Automatic Gamma Counter (PerkinElmer). Percent lysis was calculated by: $Specific\ Lysis\ (\%) = \frac{CPM - \overline{SR}}{\overline{MR} - \overline{SR}} \times 100\%$ | CPM: Counts per minute (CPM); SR: CPM of spontaneous release; MR: CPM of maximum release. Individual experiments represent the mean ± s.d. of triplicate samples from a single T cell donor. A paired Student's t-test was performed comparing experimental conditions with corresponding controls. Experiments were generally repeated with at T cells from at least three different donors.

Generation of knock-out cell lines

FACS-sorted, stable Z-138-CD19-KO and Nalm-6-CD19-KO were generated using CD19-CRISPR/Cas9 and RFP reporter gene containing homologous directed repair (HDR) Plasmid Systems (Santa Cruz Biotechnology) according to the manufacturer's directions. Briefly, DNA-In Transfection Reagent (MTI-GlobalStem) was used to transfect the plasmid system. RFP-positive cells were sorted by FACS and expanded. A stable CD19-deficient clone was verified by flow cytometry and Western blots for CD19 knock-out prior to banking for subsequent studies.

CRISPR-mediated gene editing and CD19 gRNA cloning

Patient-derived, pre-B ALL cells (LAX7D, Müschen Lab) were transduced with lentivirus expressing Lenti-dCas9-KRAB-blast (Addgene, Plasmid #89567). Blasticidin-resistant cells were subsequently transduced

with lentivirus expressing gRNAs against human CD19 in a puromycin-RFP vector backbone. gRNA sequences against human CD19 were selected from the hCRISPRi-v2 library and purchased from Integrated DNA Technologies Inc. Sequences were cloned into plasmids and verified by Sanger sequencing prior to lentivirus production. Non-targeting gRNA was used as control. 10 days post-CD19-gRNA transduction, cells were sorted based on RFP using BD Fusion.

***In vivo* tumor modeling**

Tumor models: Stable, luciferase-expressing tumor lines were established for bioluminescent imaging in mouse models. Briefly, a luciferase gene was introduced into tumor lines by a lentivirus gene delivery system (pLenti7.3/V5-DEST Gateway Vector Kit, Invitrogen). The minimum lethal dose was determined for each tumor cell line by dose titration (1.5×10^6 JeKo-1, 10 d; 0.5×10^6 Raji, 7 d; 5×10^4 Z-138-CD19-KO, 11 d; 5×10^4 Z-138-WT + 5×10^4 Z-138-CD19-KO (1:1 mixture), 8 d; and 0.2×10^6 Nalm-6-CD19-KO, 10 d). Tumor cells were injected intravenously (IV) into six- to eight-week-old NSG mice, and tumor development was daily monitored by *in vivo* bioluminescence imaging.

Bioluminescent imaging: Mice were anesthetized with isoflurane and administered 150 mg/kg D-luciferin (Life Technologies) via intraperitoneal (IP) injection 10 min prior to imaging. Imaging was performed on an AmiX imaging system (Spectral Instruments Imaging).

In vivo CAR T-cell therapy: 8-12 week old mice (n=5 per group) were challenged with the minimum lethal dose of tumor cells administered IV and then treated with CAR T cells once tumor engraftment was confirmed via imaging. Treatments consisted of a single 300 µL IV injection with defined populations of CD4 and CD8 CAR-T cells. Total CAR-positive cells infused ranged from $2\text{-}5 \times 10^6$ cells at CD4:CD8 ratio of 1:1 to 2.5:1. Controls included non-transduced T cells (Non-CAR) from the same donor and PBS.

Imaging was performed weekly up to 80 days. Survival data are reported in Kaplan-Meier plots and analyzed by log-rank tests.

Post-mortem tumor analysis: Spleens from mice challenged with Z-138-WT + Z-138-CD19KO mixture (Fig. 3d) were harvested immediately post-mortem. Spleens were prepared into a single-cell suspension by mechanical disruption and stained for human tumor cells with FACS antibodies for human CD45 APC Cy7, CD20 PerCP Cy5.5, and CD19 APC antibodies (BD Biosciences). The average percentages of CD19-positive and -negative expression in tumor cells were calculated.

Primary sample immunophenotyping

T cells were removed from thawed primary patient samples with the Human CD3 Positive Selection Kit (Stemcell Technologies). Remaining cells were stained with CD20 FITC, CD10 PEcy7, CD22 PerCP Cy5.5, CD19 PE, and BAFFR Alexa 647 antibodies (BD Biosciences). Samples were run on the BD LSRFortessa and analyzed with Flowjo Software.

Degranulation assay

1×10^5 T-cell depleted, primary patient samples were co-incubated with 2×10^5 CAR-T cells at an E:T ratio of 2:1 in complete RPMI 1640 medium containing GolgiStop Protein Transport Inhibitor reagent (BD Bioscience) and CD107a APC antibody (Biolegend) for 6 h. The cells were subsequently stained with antibodies against human CD3 Viogreen (Miltenyi Biotec), human CD19 PE-Cy7 (Biolegend), and human CD8 APC-Cy7 (Biolegend). Samples were analyzed with MACSQuant and FCS express software (Miltenyi Biotec Inc.). Non-transduced T cells from the same donors (non-CAR) were used as negative effector cells.

Intracellular cytokine production

A total of 2×10^5 CAR T cells were co-cultured overnight with 1×10^5 T cell-depleted patient sample as blast cells in 96-well tissue culture plates in the presence of Brefeldin A (BD Biosciences). The cell mixture was then stained using anti-CD8, anti-CD4, and biotinylated erbitux/streptavidin to analyze surface co-expression of CD8, CD4, and CAR, respectively. Cells were then fixed and permeabilized using the BD Cytofix/Cytoperm kit (BD Biosciences). After fixation, the T cells were stained with antibodies against IFN-γ and TNF-α. Cells were then analyzed using multicolor flow cytometry on MACSQuant and FCS express software (Miltenyi Biotec Inc.). Non-transduced T cells from the same donors (non-CAR) were used as negative effector cells.

***In vivo* patient derived xenograft (PDX) model**

$1x10^6$ leukemic cells isolated from a patient relapsing with CD19 negative B-ALL leukemia (identified by: human $CD45^+TdT^+CD79a^+CD22^+$) were injected into the tail vein of six- to eight-week-old NSG mice. Successful engraftment was determined when the percentage of peripheral blood circulating B-ALL reached 1-5% of the total (human/mouse) cells. Mice received a single infusion of $5x10^6$ CAR T cells (BAFF-R CAR or CD19 CAR, CD4/CD8 ratio 1:1) by tail vein injection. Controls included non-transduced T cells (Non-CAR) from the same donor and PBS. CAR T and leukemic cells were monitored by blood collections and FACS analysis for human $CD45^+CD3^+CD4^+CD8^+$ and $CD45^+CD22^+CD58^+$ and respectively. Circulating murine cells were determined using anti-murine CD45 antibody (Pe-Cy7-A). Data are reported as means ± SD and analyzed by a Student's t-test. Survival data is reported in a Kaplan-Meier plot analyzed by log-rank test.

Statistical analysis

All statistical analyses were performed with GraphPad Prism software. Depending on the experiment design, the following methods were used to calculate significance: Student's T test, one-way ANOVA, two-way ANOVA, two-way RM ANOVA, and log-rank tests. ANOVA tests were followed by an appropriate Tukey's, Dunnett's, or Sidak's post hoc test for multiple comparisons between experimental groups. All testing was two sided with a testing level (α) of 0.05. Unless otherwise stated, data are presented as means ± s.d., with n=3 or 4 replicates.

List of Supplementary Materials

- Fig. S1. Cytokine release assay.
- Fig. S2. BAFF-R CAR-T cell *in vitro* CTL assay.
- Fig. S3. Preliminary BAFF-R CAR-T cell assessment *in vivo*.
- Fig. S4. CAR-T cells validated for CAR expression and CTL activity.
- Fig. S5. CD19-KO clone selection.
- Data File S1. Primary data

References and Notes

1. J. N. Brudno, J. N. Kochenderfer, Chimeric antigen receptor T-cell therapies for lymphoma. *Nature reviews. Clinical oncology* **15**, 31-46 (2018).
2. D. Sommermeyer, T. Hill, S. M. Shamah, A. I. Salter, Y. Chen, K. M. Mohler, S. R. Riddell, Fully human CD19-specific chimeric antigen receptors for T-cell therapy. *Leukemia* **31**, 2191-2199 (2017).
3. J. H. Park, I. Riviere, M. Gonen, X. Wang, B. Senechal, K. J. Curran, C. Sauter, Y. Wang, B. Santomasso, E. Mead, M. Roshal, P. Maslak, M. Davila, R. J. Brentjens, M. Sadelain, Long-Term Follow-up of CD19 CAR Therapy in Acute Lymphoblastic Leukemia. *The New England journal of medicine* **378**, 449-459 (2018).
4. S. L. Maude, N. Frey, P. A. Shaw, R. Aplenc, D. M. Barrett, N. J. Bunin, A. Chew, V. E. Gonzalez, Z. Zheng, S. F. Lacey, Y. D. Mahnke, J. J. Melenhorst, S. R. Rheingold, A. Shen, D. T. Teachey, B. L. Levine, C. H. June, D. L. Porter, S. A. Grupp, Chimeric antigen receptor T cells for sustained remissions in leukemia. *The New England journal of medicine* **371**, 1507-1517 (2014).
5. X. Wang, L. L. Popplewell, J. R. Wagner, A. Naranjo, M. S. Blanchard, M. R. Mott, A. P. Norris, C. W. Wong, R. Z. Urak, W. C. Chang, S. K. Khaled, T. Siddiqi, L. E. Budde, J. Xu, B. Chang, N. Gidwaney, S. H. Thomas, L. J. Cooper, S. R. Riddell, C. E. Brown, M. C. Jensen, S. J. Forman, Phase 1 studies of central memory-derived CD19 CAR T-cell therapy following autologous HSCT in patients with B-cell NHL. *Blood* **127**, 2980-2990 (2016).
6. M. Ruella, D. M. Barrett, S. S. Kenderian, O. Shestova, T. J. Hofmann, J. Perazzelli, M. Klichinsky, V. Aikawa, F. Nazimuddin, M. Kozlowski, J. Scholler, S. F. Lacey, J. J. Melenhorst, J. J. Morrissette, D. A. Christian, C. A. Hunter, M. Kalos, D. L. Porter, C. H. June, S. A. Grupp, S. Gill, Dual CD19 and CD123 targeting prevents antigen-loss relapses after CD19-directed immunotherapies. *The Journal of clinical investigation* **126**, 3814-3826 (2016).
7. E. Sotillo, D. M. Barrett, K. L. Black, A. Bagashev, D. Oldridge, G. Wu, R. Sussman, C. Lanauze, M. Ruella, M. R. Gazzara, N. M. Martinez, C. T. Harrington, E. Y. Chung, J. Perazzelli, T. J. Hofmann, S. L. Maude, P. Raman, A. Barrera, S. Gill, S. F. Lacey, J. J. Melenhorst, D. Allman, E. Jacoby, T. Fry, C. Mackall, Y. Barash, K. W. Lynch, J. M. Maris, S. A. Grupp, A. Thomas-Tikhonenko, Convergence of Acquired Mutations and Alternative Splicing of CD19 Enables Resistance to CART-19 Immunotherapy. *Cancer discovery* **5**, 1282-1295 (2015).
8. J. M. Hildebrand, Z. Luo, M. K. Manske, T. Price-Troska, S. C. Ziesmer, W. Lin, B. S. Hostager, S. L. Slager, T. E. Witzig, S. M. Ansell, J. R. Cerhan, G. A. Bishop, A. J. Novak, A BAFF-R mutation associated with non-Hodgkin lymphoma alters TRAF recruitment and reveals new insights into BAFF-R signaling. *The Journal of experimental medicine* **207**, 2569-2579 (2010).
9. J. S. Thompson, S. A. Bixler, F. Qian, K. Vora, M. L. Scott, T. G. Cachero, C. Hession, P. Schneider, I. D. Sizing, C. Mullen, K. Strauch, M. Zafari, C. D. Benjamin, J. Tschopp, J. L. Browning, C. Ambrose, BAFF-R, a newly identified TNF receptor that specifically interacts with BAFF. *Science* **293**, 2108-2111 (2001).
10. A. J. Novak, D. M. Grote, M. Stenson, S. C. Ziesmer, T. E. Witzig, T. M. Habermann, B. Harder, K. M. Ristow, R. J. Bram, D. F. Jelinek, J. A. Gross, S. M. Ansell, Expression of BLyS and its receptors in B-cell non-Hodgkin lymphoma: correlation with disease activity and patient outcome. *Blood* **104**, 2247-2253 (2004).
11. C. V. Lee, S. G. Hymowitz, H. J. Wallweber, N. C. Gordon, K. L. Billeci, S. P. Tsai, D. M. Compaan, J. Yin, Q. Gong, R. F. Kelley, L. E. DeForge, F. Martin, M. A. Starovasnik, G. Fuh, Synthetic anti-BR3

antibodies that mimic BAFF binding and target both human and murine B cells. *Blood* **108**, 3103-3111 (2006).

12. R. Parameswaran, M. Lim, F. Fei, H. Abdel-Azim, A. Arutyunyan, I. Schiffer, M. E. McLaughlin, H. Gram, H. Huet, J. Groffen, N. Heisterkamp, Effector-mediated eradication of precursor B acute lymphoblastic leukemia with a novel Fc-engineered monoclonal antibody targeting the BAFF-R. *Molecular cancer therapeutics* **13**, 1567-1577 (2014).
13. H. Qin, G. Wei, I. Sakamaki, Z. Dong, W. A. Cheng, D. L. Smith, F. Wen, H. Sun, K. Kim, S. Cha, L. Bover, S. S. Neelapu, L. W. Kwak, Novel BAFF-Receptor Antibody to Natively Folded Recombinant Protein Eliminates Drug-Resistant Human B-cell Malignancies In Vivo. *Clinical cancer research : an official journal of the American Association for Cancer Research* **24**, 1114-1123 (2018).
14. X. Wang, A. Naranjo, C. E. Brown, C. Bautista, C. W. Wong, W. C. Chang, B. Aguilar, J. R. Ostberg, S. R. Riddell, S. J. Forman, M. C. Jensen, Phenotypic and functional attributes of lentivirus-modified CD19-specific human CD8+ central memory T cells manufactured at clinical scale. *Journal of immunotherapy* **35**, 689-701 (2012).
15. X. Wang, C. Berger, C. W. Wong, S. J. Forman, S. R. Riddell, M. C. Jensen, Engraftment of human central memory-derived effector CD8+ T cells in immunodeficient mice. *Blood* **117**, 1888-1898 (2011).
16. M. Sabatino, J. Hu, M. Sommariva, S. Gautam, V. Fellowes, J. D. Hocker, S. Dougherty, H. Qin, C. A. Klebanoff, T. J. Fry, R. E. Gress, J. N. Kochenderfer, D. F. Stroncek, Y. Ji, L. Gattinoni, Generation of clinical-grade CD19-specific CAR-modified CD8+ memory stem cells for the treatment of human B-cell malignancies. *Blood* **128**, 519-528 (2016).
17. C. S. Hinrichs, Z. A. Borman, L. Gattinoni, Z. Yu, W. R. Burns, J. Huang, C. A. Klebanoff, L. A. Johnson, S. P. Kerkar, S. Yang, P. Muranski, D. C. Palmer, C. D. Scott, R. A. Morgan, P. F. Robbins, S. A. Rosenberg, N. P. Restifo, Human effector CD8+ T cells derived from naive rather than memory subsets possess superior traits for adoptive immunotherapy. *Blood* **117**, 808-814 (2011).
18. M. Schmueck-Henneresse, B. Omer, T. Shum, H. Tashiro, M. Mamonkin, N. Lapteva, S. Sharma, L. Rollins, G. Dotti, P. Reinke, H. D. Volk, C. M. Rooney, Comprehensive Approach for Identifying the T Cell Subset Origin of CD3 and CD28 Antibody-Activated Chimeric Antigen Receptor-Modified T Cells. *Journal of immunology* **199**, 348-362 (2017).
19. L. Gattinoni, E. Lugli, Y. Ji, Z. Pos, C. M. Paulos, M. F. Quigley, J. R. Almeida, E. Gostick, Z. Yu, C. Carpenito, E. Wang, D. C. Douek, D. A. Price, C. H. June, F. M. Marincola, M. Roederer, N. P. Restifo, A human memory T cell subset with stem cell-like properties. *Nature medicine* **17**, 1290-1297 (2011).
20. S. J. Schuster, J. Svoboda, E. A. Chong, S. D. Nasta, A. R. Mato, O. Anak, J. L. Brogdon, I. Pruteanu-Malinici, V. Bhoj, D. Landsburg, M. Wasik, B. L. Levine, S. F. Lacey, J. J. Melenhorst, D. L. Porter, C. H. June, Chimeric Antigen Receptor T Cells in Refractory B-Cell Lymphomas. *The New England journal of medicine* **377**, 2545-2554 (2017).
21. S. Shojaee, R. Caeser, M. Buchner, E. Park, S. Swaminathan, C. Hurtz, H. Geng, L. N. Chan, L. Klemm, W. K. Hofmann, Y. H. Qiu, N. Zhang, K. R. Coombes, E. Paietta, J. Molkentin, H. P. Koeffler, C. L. Willman, S. P. Hunger, A. Melnick, S. M. Kornblau, M. Muschen, Erk Negative Feedback Control Enables Pre-B Cell Transformation and Represents a Therapeutic Target in Acute Lymphoblastic Leukemia. *Cancer cell* **28**, 114-128 (2015).
22. S. Xie, J. Duan, B. Li, P. Zhou, G. C. Hon, Multiplexed Engineering and Analysis of Combinatorial Enhancer Activity in Single Cells. *Molecular cell* **66**, 285-299 e285 (2017).

23. M. A. Horlbeck, L. A. Gilbert, J. E. Villalta, B. Adamson, R. A. Pak, Y. Chen, A. P. Fields, C. Y. Park, J. E. Corn, M. Kampmann, J. S. Weissman, Compact and highly active next-generation libraries for CRISPR-mediated gene repression and activation. *eLife* **5**, (2016).
24. H. Kantarjian, A. Stein, N. Gokbuget, A. K. Fielding, A. C. Schuh, J. M. Ribera, A. Wei, H. Dombret, R. Foa, R. Bassan, O. Arslan, M. A. Sanz, J. Bergeron, F. Demirkan, E. Lech-Maranda, A. Rambaldi, X. Thomas, H. A. Horst, M. Bruggemann, W. Klapper, B. L. Wood, A. Fleishman, D. Nagorsen, C. Holland, Z. Zimmerman, M. S. Topp, Blinatumomab versus Chemotherapy for Advanced Acute Lymphoblastic Leukemia. *The New England journal of medicine* **376**, 836-847 (2017).
25. L. Fu, Y. C. Lin-Lee, L. V. Pham, A. T. Tamayo, L. C. Yoshimura, R. J. Ford, BAFF-R promotes cell proliferation and survival through interaction with IKKbeta and NF-kappaB/c-Rel in the nucleus of normal and neoplastic B-lymphoid cells. *Blood* **113**, 4627-4636 (2009).
26. L. V. Pham, L. Fu, A. T. Tamayo, C. Bueso-Ramos, E. Drakos, F. Vega, L. J. Medeiros, R. J. Ford, Constitutive BR3 receptor signaling in diffuse, large B-cell lymphomas stabilizes nuclear factor-kappaB-inducing kinase while activating both canonical and alternative nuclear factor-kappaB pathways. *Blood* **117**, 200-210 (2011).
27. Y. J. Li, W. Q. Jiang, H. L. Rao, J. J. Huang, Y. Xia, H. Q. Huang, T. Y. Lin, Z. J. Xia, S. Li, Z. M. Li, Expression of BAFF and BAFF-R in follicular lymphoma: correlation with clinicopathologic characteristics and survival outcomes. *PloS one* **7**, e50936 (2012).
28. X. Shen, M. Wang, Y. Guo, S. Ju, The Correlation Between Non-Hodgkin Lymphoma and Expression Levels of B-Cell Activating Factor and Its Receptors. *Advances in clinical and experimental medicine : official organ Wroclaw Medical University* **25**, 837-844 (2016).
29. R. Parameswaran, M. Muschen, Y. M. Kim, J. Groffen, N. Heisterkamp, A functional receptor for B-cell-activating factor is expressed on human acute lymphoblastic leukemias. *Cancer research* **70**, 4346-4356 (2010).
30. D. J. Miller, C. E. Hayes, Phenotypic and genetic characterization of a unique B lymphocyte deficiency in strain A/WySnJ mice. *European journal of immunology* **21**, 1123-1130 (1991).
31. Y. Sasaki, S. Casola, J. L. Kutok, K. Rajewsky, M. Schmidt-Supprian, TNF family member B cell-activating factor (BAFF) receptor-dependent and -independent roles for BAFF in B cell physiology. *Journal of immunology* **173**, 2245-2252 (2004).
32. S. J. Rodig, A. Shahsafaei, B. Li, C. R. Mackay, D. M. Dorfman, BAFF-R, the major B cell-activating factor receptor, is expressed on most mature B cells and B-cell lymphoproliferative disorders. *Human pathology* **36**, 1113-1119 (2005).
33. N. Nakamura, H. Hase, D. Sakurai, S. Yoshida, M. Abe, N. Tsukada, J. Takizawa, S. Aoki, M. Kojima, S. Nakamura, T. Kobata, Expression of BAFF-R (BR 3) in normal and neoplastic lymphoid tissues characterized with a newly developed monoclonal antibody. *Virchows Archiv : an international journal of pathology* **447**, 53-60 (2005).
34. J. C. Paterson, S. Tedoldi, A. Craxton, M. Jones, M. L. Hansmann, G. Collins, H. Roberton, Y. Natkunam, S. Pileri, E. Campo, E. A. Clark, D. Y. Mason, T. Marafioti, The differential expression of LCK and BAFF-receptor and their role in apoptosis in human lymphomas. *Haematologica* **91**, 772-780 (2006).
35. A. Davidson, Targeting BAFF in autoimmunity. *Current opinion in immunology* **22**, 732-739 (2010).
36. R. Furie, M. Petri, O. Zamani, R. Cervera, D. J. Wallace, D. Tegzova, J. Sanchez-Guerrero, A. Schwarting, J. T. Merrill, W. W. Chatham, W. Stohl, E. M. Ginzler, D. R. Hough, Z. J. Zhong, W. Freimuth, R. F. van Vollenhoven, B.-S. Group, A phase III, randomized, placebo-controlled study of belimumab, a monoclonal antibody that inhibits B lymphocyte stimulator, in patients with systemic lupus erythematosus. *Arthritis and rheumatism* **63**, 3918-3930 (2011).

37. G. Fazio, N. Turazzi, V. Cazzaniga, M. Kreuzaler, O. Maglia, C. F. Magnani, E. Biagi, A. Rolink, A. Biondi, G. Cazzaniga, TNFRSF13C (BAFFR) positive blasts persist after early treatment and at relapse in childhood B-cell precursor acute lymphoblastic leukaemia. *British journal of haematology* **182**, 434-436 (2018).
38. E. M. McWilliams, C. R. Lucas, T. Chen, B. K. Harrington, R. Wasmuth, A. Campbell, K. A. Rogers, C. M. Cheney, X. Mo, L. A. Andritsos, F. T. Awan, J. Woyach, W. E. Carson, 3rd, J. Butchar, S. Tridandapani, E. Hertlein, C. E. Castro, N. Muthusamy, J. C. Byrd, Anti-BAFF-R antibody VAY-736 demonstrates promising preclinical activity in CLL and enhances effectiveness of ibrutinib. *Blood advances* **3**, 447-460 (2019).
39. N. Turazzi, G. Fazio, V. Rossi, A. Rolink, G. Cazzaniga, A. Biondi, C. F. Magnani, E. Biagi, Engineered T cells towards TNFRSF13C (BAFFR): a novel strategy to efficiently target B-cell acute lymphoblastic leukaemia. *British journal of haematology* **182**, 939-943 (2018).
40. M. Ruella, M. V. Maus, Catch me if you can: Leukemia Escape after CD19-Directed T Cell Immunotherapies. *Computational and structural biotechnology journal* **14**, 357-362 (2016).
41. T. J. Fry, N. N. Shah, R. J. Orentas, M. Stetler-Stevenson, C. M. Yuan, S. Ramakrishna, P. Wolters, S. Martin, C. Delbrook, B. Yates, H. Shalabi, T. J. Fountaine, J. F. Shern, R. G. Majzner, D. F. Stroncek, M. Sabatino, Y. Feng, D. S. Dimitrov, L. Zhang, S. Nguyen, H. Qin, B. Dropulic, D. W. Lee, C. L. Mackall, CD22-targeted CAR T cells induce remission in B-ALL that is naive or resistant to CD19-targeted CAR immunotherapy. *Nature medicine* **24**, 20-28 (2018).
42. N. N. Shah, M. S. Stevenson, C. M. Yuan, K. Richards, C. Delbrook, R. J. Kreitman, I. Pastan, A. S. Wayne, Characterization of CD22 expression in acute lymphoblastic leukemia. *Pediatric blood & cancer* **62**, 964-969 (2015).
43. J. Rosenthal, A. S. Naqvi, G. Wertheim, M. Paessler, S. R. Rheingold, A. Thomas-Tikhonenko, V. Pillai, Semi-Quantitative Analysis of CD19 and CD22 Expression in B-Lymphoblastic Leukemia and Implications for Targerted Immunotherapy. *Blood* **130**, 1331-1331 (2017).

Acknowledgements:

Research reported in this publication included work performed in the Analytical Cytometry Core, Hematopoietic Tissue Biorepository Core, Integrative Genomics Core, and Small Animal Imaging Core supported by the National Cancer Institute of the National Institutes of Health under award number P30CA033572. The content is solely the responsibility of the authors and does not necessarily represent the official views of the National Institutes of Health. We thank the Sandra and Edward Meyer Cancer Center PDTX Shared Resource for their support. **Funding:** We are grateful for the generous support from the Toni Stephenson Lymphoma Center at Beckman Research Institute of City of Hope. The study was also supported by: the Leukemia and Lymphoma Society (LLS): Translational Research Program (TRP 6540-18; PI: L.W.K.), Mantle cell lymphoma Research Initiative (MCL 7000-18; PI: L.W.K.), and SCOR grants (SCOR 7011-16 and 7012-16; PI: G.G.I.); the NIH/NCI (SPORE 2P50CA107399; PI: S.J.F. and L.W.K. ; 1R21CA223141; PI: H.Q), Department of Defense (CA170783; PI: L.W.K) and the Hope Portfolio Fund at City of Hope (PI: H.Q.). **Author contributions:** H.Q. Designed the project, oversaw experiments, analyzed data, and wrote the manuscript. Z.D., F.W., W.X., and H.S. conducted *in vitro* and *in vivo* experiments. X.W. and M.W. developed and conducted CAR-T cell degranulation and activation assays. W.A.C. and D.L.S. contributed to data analysis and manuscript preparation. G.W. and X.S. developed the BAFF-R scFv. F.F. and J.X. developed and conducted surface antigen density assays. T.I.P., C.C., C.K., L.S., and G.G.I. developed PDX models. J.Y.S. and I.A. provided primary tumor samples. M.M., S.J.F., and L.W.K. oversaw the project including data analysis and manuscript writing. **Competing interests:** L.W.K. and H.Q. are inventors on patents WO2017214167 and WO 2017214170, submitted by City of Hope, which is related to this work. L.W.K. – InnoLifes: Consultancy, Equity Ownership; Pepromene Bio: Consultancy, Equity Ownership. H.Q. – InnoLifes: Consultancy, Equity Ownership; Pepromene Bio: Consultancy, Equity Ownership. The other authors do not declare competing interests. **Data and materials availability:** All data associated with this study are present in the paper or Supplementary Materials. Materials

produced in this study are protected by City of Hope intellectual property patents but will remain available to qualified investigators at other research organization by establishing a Material Transfer Agreement and in accordance with the NIH Principles and Guidelines.

Figure legends:

Figure 1. BAFF-R CAR-T cells activate and elicit specific cytotoxicity against multiple subtypes of human B-cell malignancies. (a) Either CD4+ or CD8+ BAFF-R CAR T cells were incubated with BAFF-R expressing L cells, mantle cell lymphoma (MCL) lines JeKo-1, Z-138, or as controls, parental L cells (mouse fibroblast) or T-activator CD3/CD28 beads. ELISA measurement of cytokines IFN-γ, TNF-α, and granzyme B supernatant concentrations were determined following 24 h of incubation with targets. **(b)** Cytotoxic T-lymphocyte assay measuring the specific lysis of target cells by chromium-51 release after 4 h. Various chromium-51 labeled BAFF-R-positive lymphoma and leukemia cell lines, BAFF-R-expressing L cells, or control BAFF-R-negative parental L cells were incubated with either CD4 or CD8 CAR T cells, as indicated at an effector-to-target ratio of 3:1. FL, follicular lymphoma; DLBCL, diffuse large B-cell lymphoma; B-ALL, B-cell acute lymphocytic leukemia; B-CLL, B-cell chronic lymphocytic leukemia. **(c)** Lymphomas from primary patient samples were labelled with chromium-51 and incubated either with naïve CD4 or CD8 BAFF-R-CAR T cells at various effector-to-target ratios as in (b). Non-transduced T cells from the same healthy donors were used as allogeneic controls (non-CAR). Data are shown as the mean ± s.d. of one CAR T-cell donor against triplicate tumors samples. All experiments were repeated with at least three different CAR T-cell donors. **P<0.001 vs. corresponding non-CAR control with the following tests: (a) One-way ANOVA and Dunnett's multiple comparisons test; (b) Two-way ANOVA and Dunnett's multiple comparisons test; (c) Two-way ANOVA and Tukey's multiple comparisons test .

Figure 2. Defined subpopulations of BAFF-R CAR-T cells eliminated established MCL tumors, *in vivo,* after a single treatment. (a) Bioluminescence images and survival of groups of 5 NSG mice following intravenous (IV) tumor challenge (10^6 cells/mouse) on day 0 with luciferase-expressing human MCL line JeKo-1. CD4 T_N CAR-T cells combined with either subpopulations of CD8 T_{CM}, T_N, or T_{SCM} CAR-T cells were infused IV on day 10 at a single dose of 10^6 CD4 T_N + 10^6 CD8 CAR-T cells. Control mice received non-transduced CD4/CD8 T cells from the same donor as an allogeneic control (Non-CAR), or PBS. **(b)** Survival data were analyzed by Kaplan-Meier plots of overall survival at 100 days. Data are representative of three independent experiments using different donor T cells. Log-rank test: **P<0.01 and *P<0.05 compared with controls.

Figure 3 Superiority of BAFF-R *versus* CD19 CAR T cells in a Burkitt lymphoma model is not due to greater tumor antigen density. (a) Bioluminescence images of groups of 5 NSG mice following IV tumor challenge (0.5 x 10^6 cells/mouse) on day 0 with luciferase-expressing Raji cells. 2.5 x 10^6 activated CD4 T_N CAR-T + 10^6 CD8 T_N BAFF-R- or CD19-CAR T cells were infused IV on day 7 as a single dose. Control mice received non-transduced CD4/CD8 T cells from the same donor as an allogeneic control, or PBS. Data are representative of two independent experiments using different donor T cells. **(b)** Kaplan-Meier plot of overall survival at 80 days is shown. Log-rank test: **P<0.01 compared with all other groups. **(c)** Calculated cell surface antigen density of BAFF-R and CD19 on lymphoma and leukemia lines stained by PE-conjugated antibodies at saturation. PE per cell (assuming 1 PE per antibody) was calculated against mean fluorescence intensity (MFI) standard curve with BD Quantibrite beads. Data are represented as mean ± s.d. of triplicates. Student's t-test: **P<0.001 BAFF-R vs. CD19 in corresponding cell line.

Figure 4. Therapeutic effects of BAFF-R CAR T cells against CD19-*negative* human tumor lines *in vitro* and *in vivo*. CD19-negative B-cell tumor variant clones were generated by CRISPR/HDR CD19 gene knock-out (KO) of **(a)** two lymphoma cell lines (Z-138, MCL; MEC-1, CLL) and **(b)** one ALL cell line (Nalm-6), or by gRNA CD19 gene knock-down (KD) of one ALL PDX. FACS histograms indicate CD19 and BAFF-R(*13*) expression on wildtype (WT) and corresponding KO/KD tumors. Cytotoxicity of corresponding tumor targets mediated by CD8 BAFF-R T_N (blue) or CD19 T_N CAR T cells (red) incubated at various effector-to-target ratios was determined by chromium-51 release by tumor targets after 4 h. Non-transduced T cells from the same donor were used as an allogeneic control (green, dotted). Data are shown as the mean ± s.d. of triplicate samples. Data are representative of at least three independent experiments using different donor T cells. Two-way ANOVA and Tukey's multiple comparisons test: **P<0.001 vs. non-CAR control. **(c-d)** Bioluminescence images of NSG mice following IV tumor challenge on day 0 with luciferase-expressing (c) 5 x 10^4 Z-138-CD19KO MCL or (d) 2 x 10^5 Nalm-6-CD19KO ALL tumors. Groups of 5 tumor-bearing mice each were then randomly assigned to treatment with either 2.5 x 10^6 CD4 T_N CAR-T + 10^6 CD8 T_N BAFF-R- or CD19-CAR T cells/mouse IV on day 11 or 10, respectively, as a single dose. Non-transduced CD4/CD8 T cells from the same donor were used as allogeneic controls (non-CAR). Data are representative of two independent experiments using different donor T cells. Kaplan-Meier plots of overall survival are shown. Log-rank test: **P<0.01 BAFF-R-CAR vs. CD19-CAR and controls.

Figure 5. BAFF-R CAR T cells eliminate pre-existing CD19 antigen loss variants *in vivo*. (a) Bioluminescence images of NSG mice following IV tumor challenge on day 0 with a mixture of 5 x 10^4 luciferase-expressing Z-138 (wildtype) plus 5 x 10^4 Z-138-CD19KO tumor cells. Groups of 5 tumor-bearing mice each were then randomly assigned to treatment with either 2.5 x 10^6 CD4 T_N CAR-T + 10^6 CD8 T_N BAFF-R- or CD19-CAR T cells/mouse IV on day 8, as a single dose. Non-transduced CD4/CD8 T cells from the same donor were used as allogeneic controls (non-CAR). **(b)** Kaplan-Meier plots of overall survival are shown. Log-rank test: **P<0.01 BAFF-R-CAR vs. CD19-CAR and controls. **(c)** Representative FACS plots of post-mortem tumor analysis from spleens of mice treated in (a). Cells were gated on $CD45^+$ human tumor cells and analyzed for CD19 expression. Summary graph of mean percentage ± s.d. of triplicate samples CD19+/- tumor cells from n=5 mice/group. ***No tumor cells were detected. Two-way ANOVA and Tukey's multiple comparisons test: **P<0.001 percentage of CD19-positive tumor cells vs. non-CAR and PBS controls.

Figure 6. BAFF-R specific activation of CAR T cells by primary CD19 antigen-loss human ALL escape variants and antitumor effects of CAR T cells *in vivo*. Blood or bone marrow tumor samples were obtained from ALL patients relapsing with CD19-negative tumors following CD19 bi-specific antibody treatment (relapse) and analyzed together with each patient's corresponding pre-therapy tumor. **(a)** FACS histograms showing expression of CD19 and BAFF-R. **(b)** Cryopreserved ALL samples were co-cultured with BAFF-R or CD19 CAR-T cells derived from a single healthy donor in the presence of anti-CD107a antibody for 6 h. Non-transduced T cells (non-CAR) from a single donor were used as a negative control. **(c)** FACS analysis of CD19-negative B-ALL cells isolated at relapse from a fifth patient for PDX establishment. B-ALL cells (10^6 cells/mouse) were injected into NSG mice, and 4 mice/group were then randomly assigned to treatments of BAFF-R-or CD19-CAR T cells (5 x 10^6, 1:1 CD4:CD8 T_N CAR T cells ratio/mouse) on day 26. Non-transduced T cells (1:1 CD4:CD8 T_N cells) from the same donor were used as allogeneic controls (non-CAR) **(d)** Percentage of peripheral blood CD19-negative B-ALL blasts in PDX mice at days 26 and 54. B-ALL blasts were identified by $CD45^+CD22^+CD58^+$ staining. Two-way, repeated measures ANOVA and Sidak's multiple comparisons test: **P<0.001 BAFF-R CAR vs. CD19-CAR and controls. **(e)** Overall survival of CD19-negative B-ALL PDX mice after BAFF-R CAR-T treatment. Control groups include CD19 CAR-T, non-transduced T cells, and PBS. Log-rank test: **P<0.01 vs. CD19-CAR, non-CAR, and PBS control.

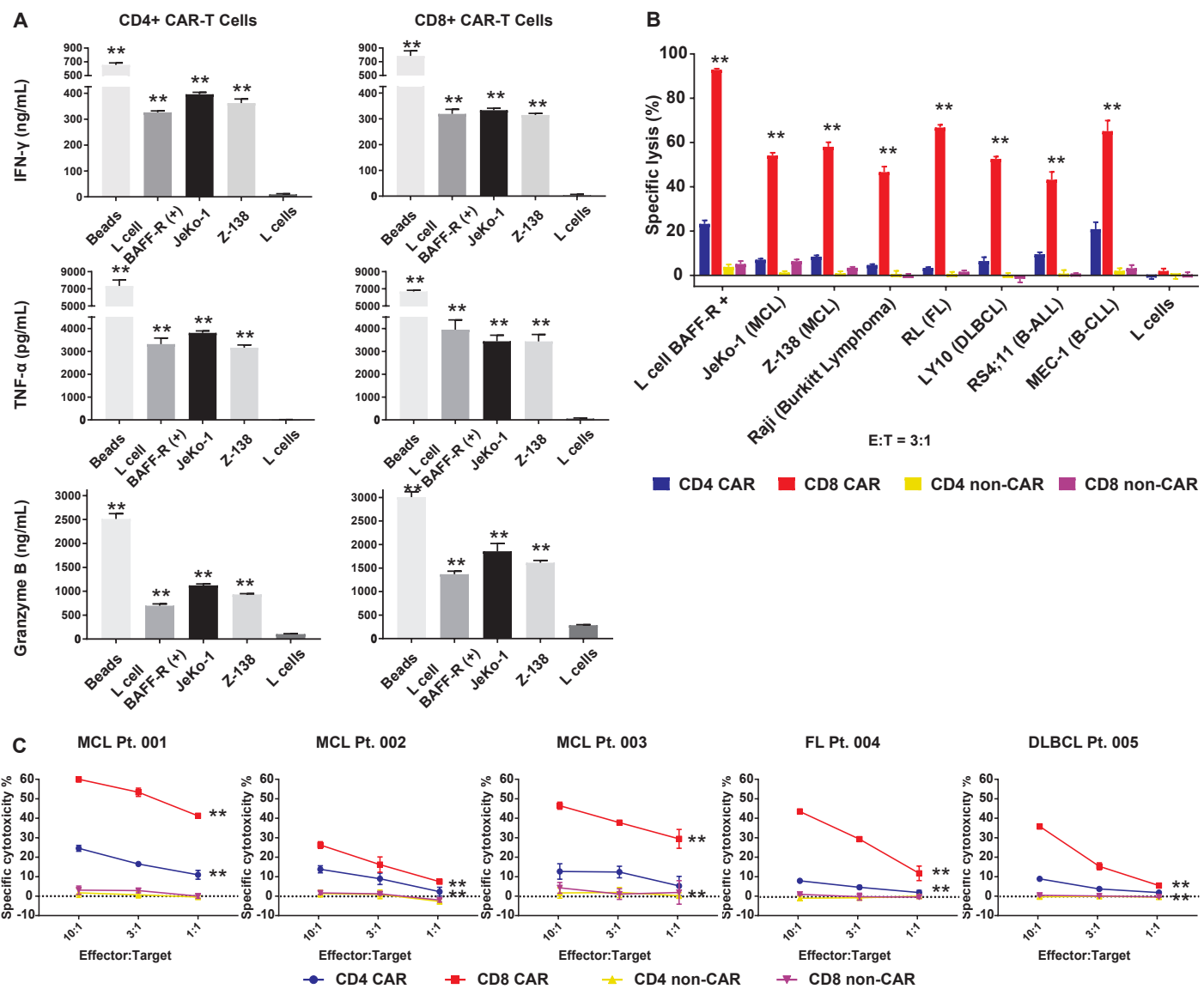
A
CD4+ CAR-T Cells
CD8+ CAR-T Cells
IFN-γ (ng/mL)
TNF-α (pg/mL)
Granzyme B (ng/mL)
Beads
L cell
BAFF-R (+)
JeKo-1
Z-138
L cells
B
Specific lysis (%)
L cell BAFF-R +
JeKo-1 (MCL)
Z-138 (MCL)
Raji (Burkitt Lymphoma)
RL (FL)
LY10 (DLBCL)
RS4;11 (B-ALL)
MEC-1 (B-CLL)
L cells
E:T = 3:1
CD4 CAR
CD8 CAR
CD4 non-CAR
CD8 non-CAR
C
MCL Pt. 001
MCL Pt. 002
MCL Pt. 003
FL Pt. 004
DLBCL Pt. 005
Specific cytotoxicity %
Effector:Target
10:1
3:1
1:1
CD4 CAR
CD8 CAR
CD4 non-CAR
CD8 non-CAR

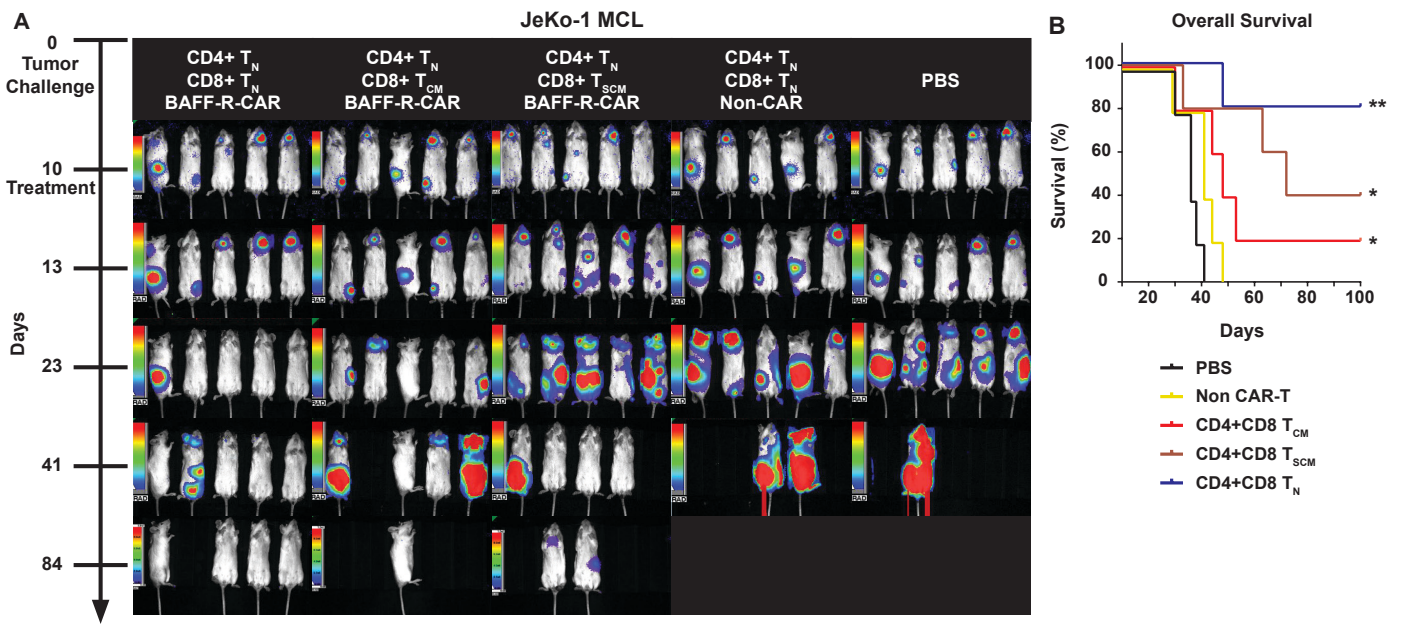
A
JeKo-1 MCL
0
Tumor Challenge
10
Treatment
13
23
41
84
Days
CD4+ T_N
CD8+ T_N
BAFF-R-CAR
CD4+ T_N
CD8+ T_{CM}
BAFF-R-CAR
CD4+ T_N
CD8+ T_{SCM}
BAFF-R-CAR
CD4+ T_N
CD8+ T_N
Non-CAR
PBS
B
Overall Survival
Survival (%)
100
80
60
40
20
0
20
40
60
80
100
Days
**
*
*
PBS
Non CAR-T
CD4+CD8 T_{CM}
CD4+CD8 T_{SCM}
CD4+CD8 T_N

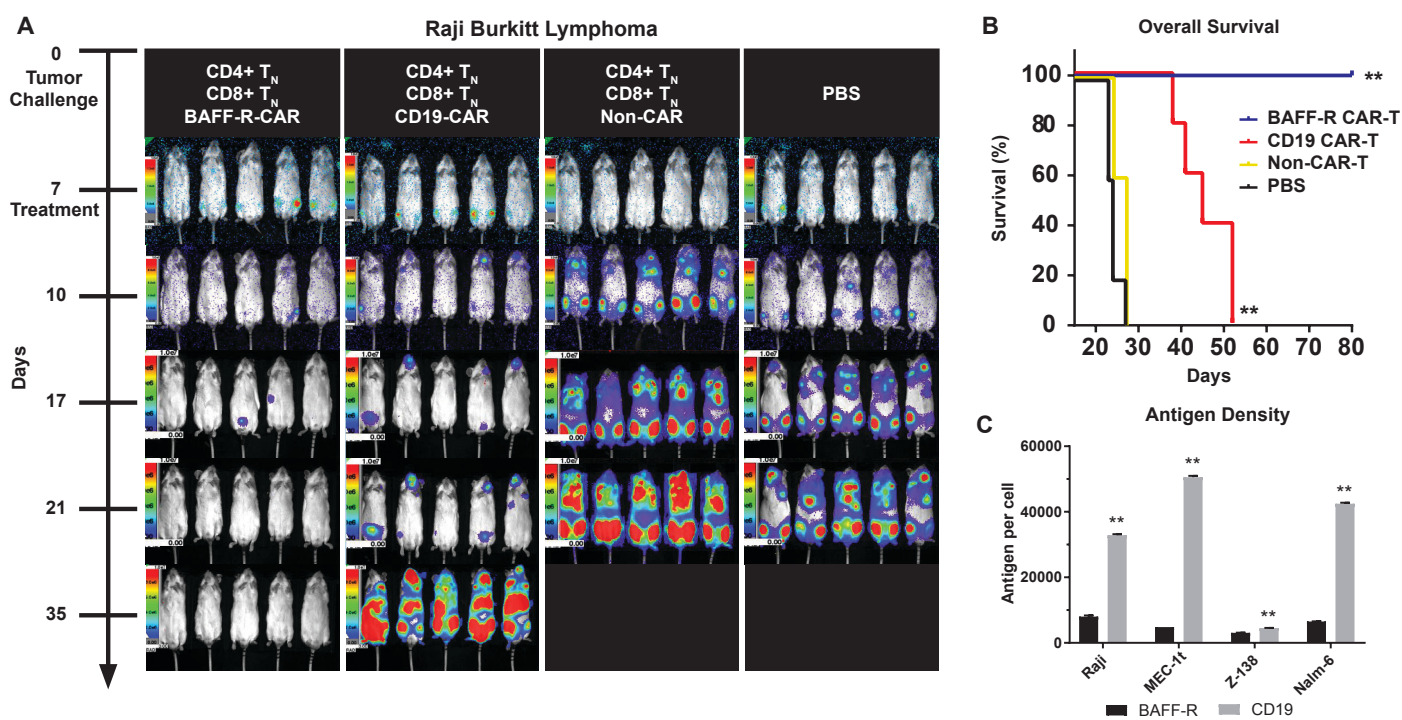
A
Raji Burkitt Lymphoma
0
Tumor Challenge
7
Treatment
10
17
21
35
Days
CD4+ T_N
CD8+ T_N
BAFF-R-CAR
CD4+ T_N
CD8+ T_N
CD19-CAR
CD4+ T_N
CD8+ T_N
Non-CAR
PBS
B
Overall Survival
Survival (%)
100
80
60
40
20
0
20 30 40 50 60 70 80
Days
**
**
BAFF-R CAR-T
CD19 CAR-T
Non-CAR-T
PBS
C
Antigen Density
Antigen per cell
60000
40000
20000
0
**
**
**
**
Raji
MEC-1t
Z-138
Nalm-6
BAFF-R
CD19

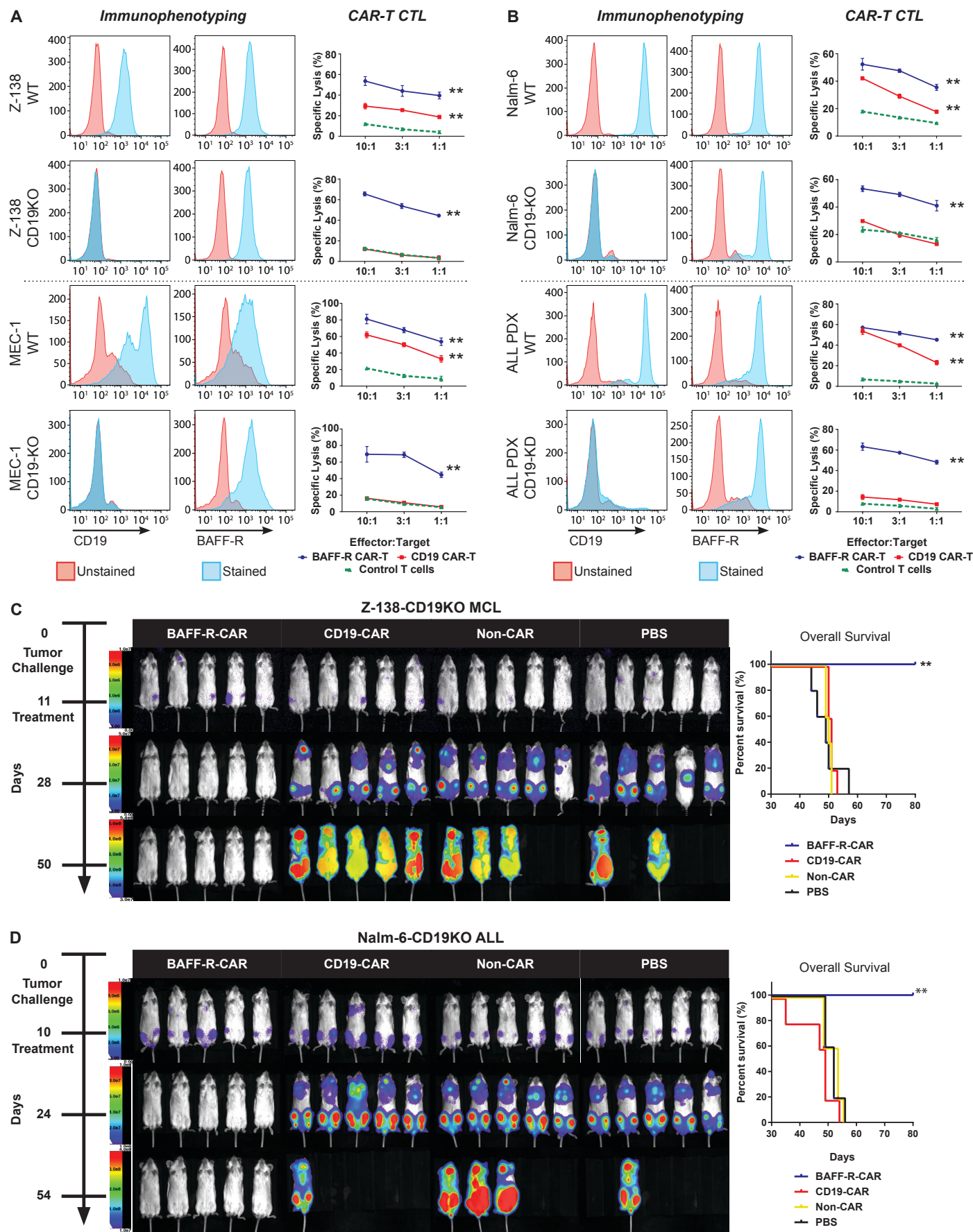
A
Immunophenotyping
CAR-T CTL
Z-138 WT
Z-138 CD19KO
MEC-1 WT
MEC-1 CD19-KO
Specific Lysis (%)
10:1
3:1
1:1
**
CD19
BAFF-R
Unstained
Stained
Effector:Target
BAFF-R CAR-T
CD19 CAR-T
Control T cells
B
Immunophenotyping
CAR-T CTL
Nalm-6 WT
Nalm-6 CD19-KO
ALL PDX WT
ALL PDX CD19-KD
C
Z-138-CD19KO MCL
BAFF-R-CAR
CD19-CAR
Non-CAR
PBS
0
Tumor Challenge
11
Treatment
Days
28
50
Overall Survival
Percent survival (%)
Days
D
Nalm-6-CD19KO ALL
0
Tumor Challenge
10
Treatment
Days
24
54
Overall Survival
Percent survival (%)
Days

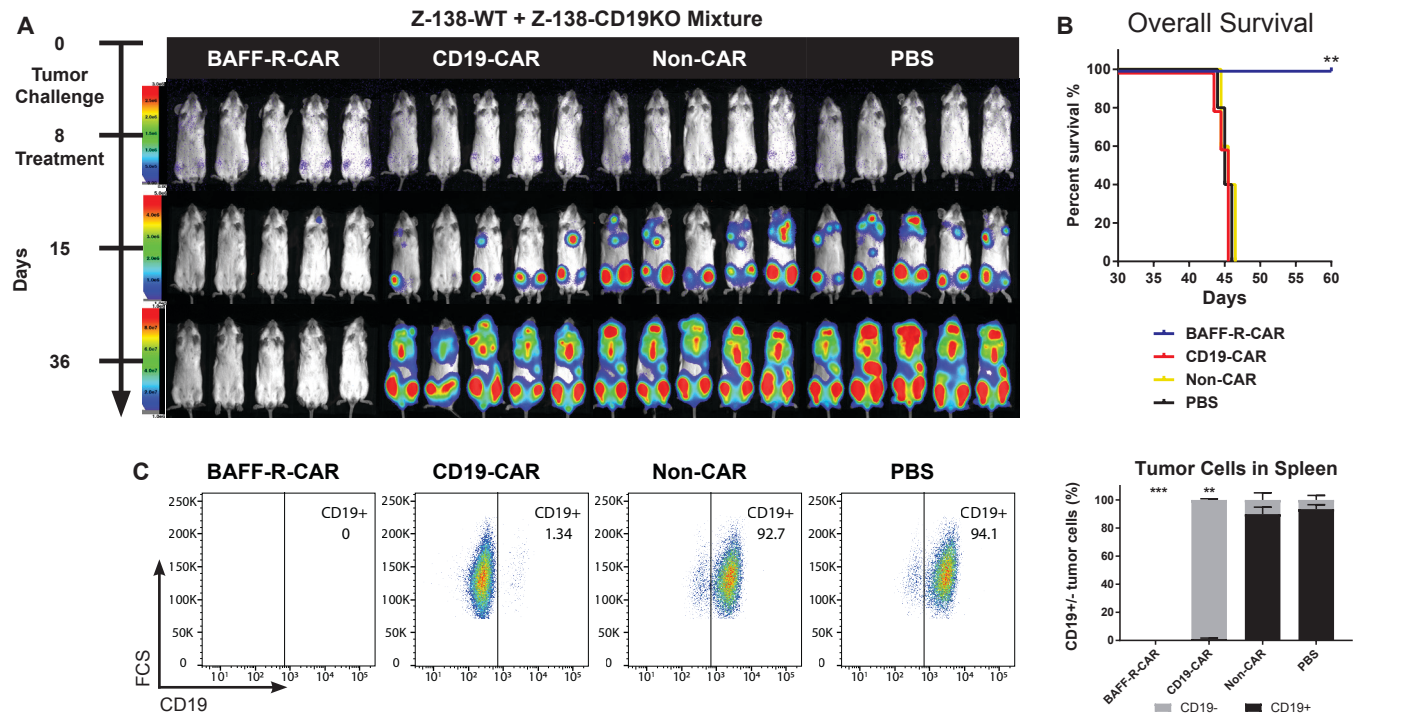
A
Z-138-WT + Z-138-CD19KO Mixture
BAFF-R-CAR
CD19-CAR
Non-CAR
PBS
0
Tumor Challenge
8
Treatment
15
36
Days
B
Overall Survival
Percent survival %
Days
**
BAFF-R-CAR
CD19-CAR
Non-CAR
PBS
C
CD19+ 0
CD19+ 1.34
CD19+ 92.7
CD19+ 94.1
FCS
CD19
Tumor Cells in Spleen
CD19+/- tumor cells (%)
***
**
CD19-
CD19+

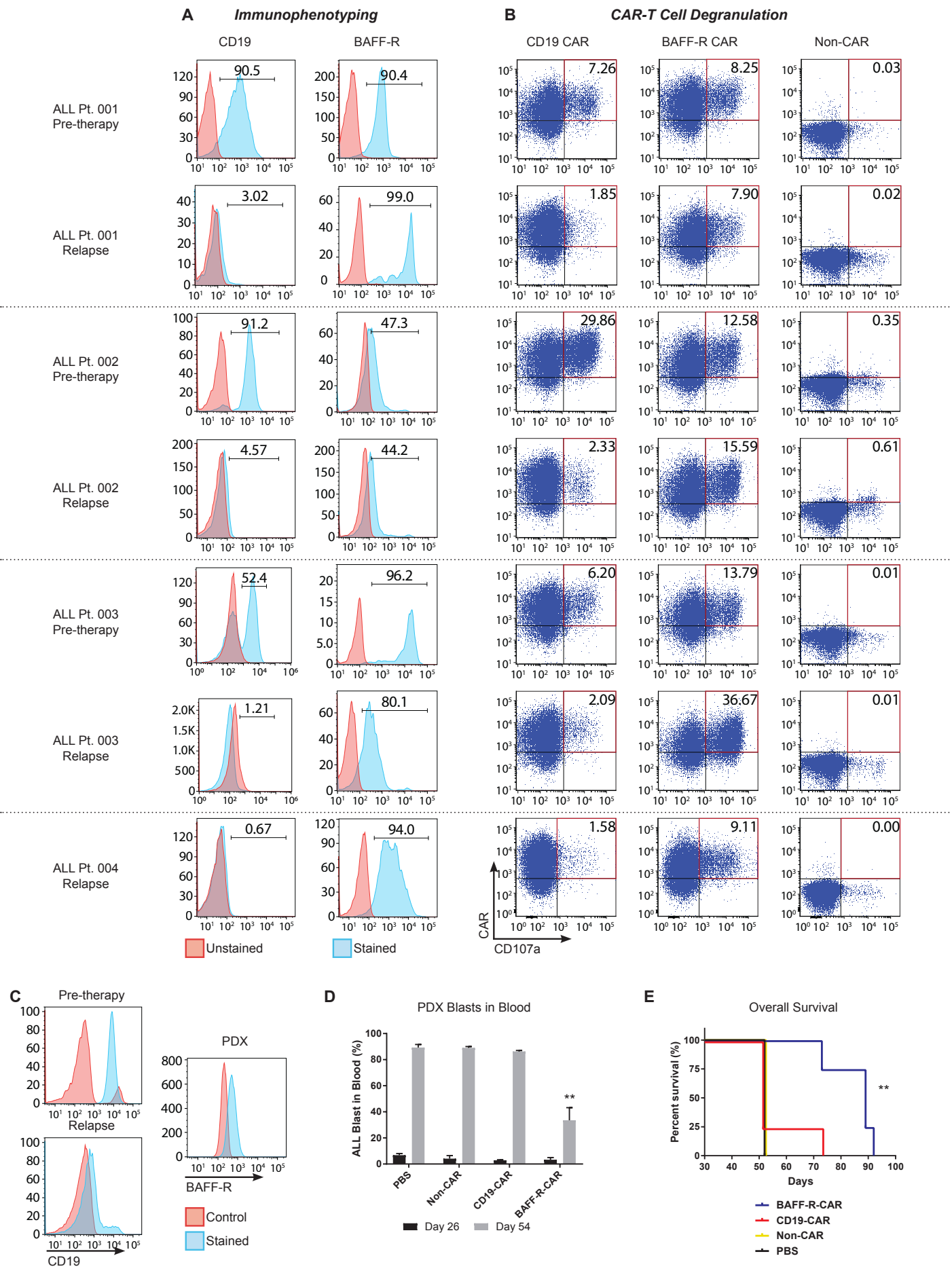
A
Immunophenotyping
CD19
BAFF-R
B
CAR-T Cell Degranulation
CD19 CAR
BAFF-R CAR
Non-CAR
ALL Pt. 001 Pre-therapy
90.5
90.4
7.26
8.25
0.03
ALL Pt. 001 Relapse
3.02
99.0
1.85
7.90
0.02
ALL Pt. 002 Pre-therapy
91.2
47.3
29.86
12.58
0.35
ALL Pt. 002 Relapse
4.57
44.2
2.33
15.59
0.61
ALL Pt. 003 Pre-therapy
52.4
96.2
6.20
13.79
0.01
ALL Pt. 003 Relapse
1.21
80.1
2.09
36.67
0.01
ALL Pt. 004 Relapse
0.67
94.0
1.58
9.11
0.00
Unstained
Stained
CAR
CD107a
C
Pre-therapy
Relapse
CD19
PDX
BAFF-R
Control
Stained
D
PDX Blasts in Blood
ALL Blast in Blood (%)
PBS
Non-CAR
CD19-CAR
BAFF-R-CAR
**
Day 26
Day 54
E
Overall Survival
Percent survival (%)
Days
**
BAFF-R-CAR
CD19-CAR
Non-CAR
PBS

Supplementary Materials

- Fig. S1. Cytokine release assay.
- Fig. S2. BAFF-R CAR-T cell *in vitro* CTL assay.
- Fig. S3. Preliminary BAFF-R CAR-T cell assessment *in vivo*.
- Fig. S4. CAR-T cells validated for CAR expression and CTL activity.
- Fig. S5. CD19-KO clone selection.
- Data File S1. Primary data

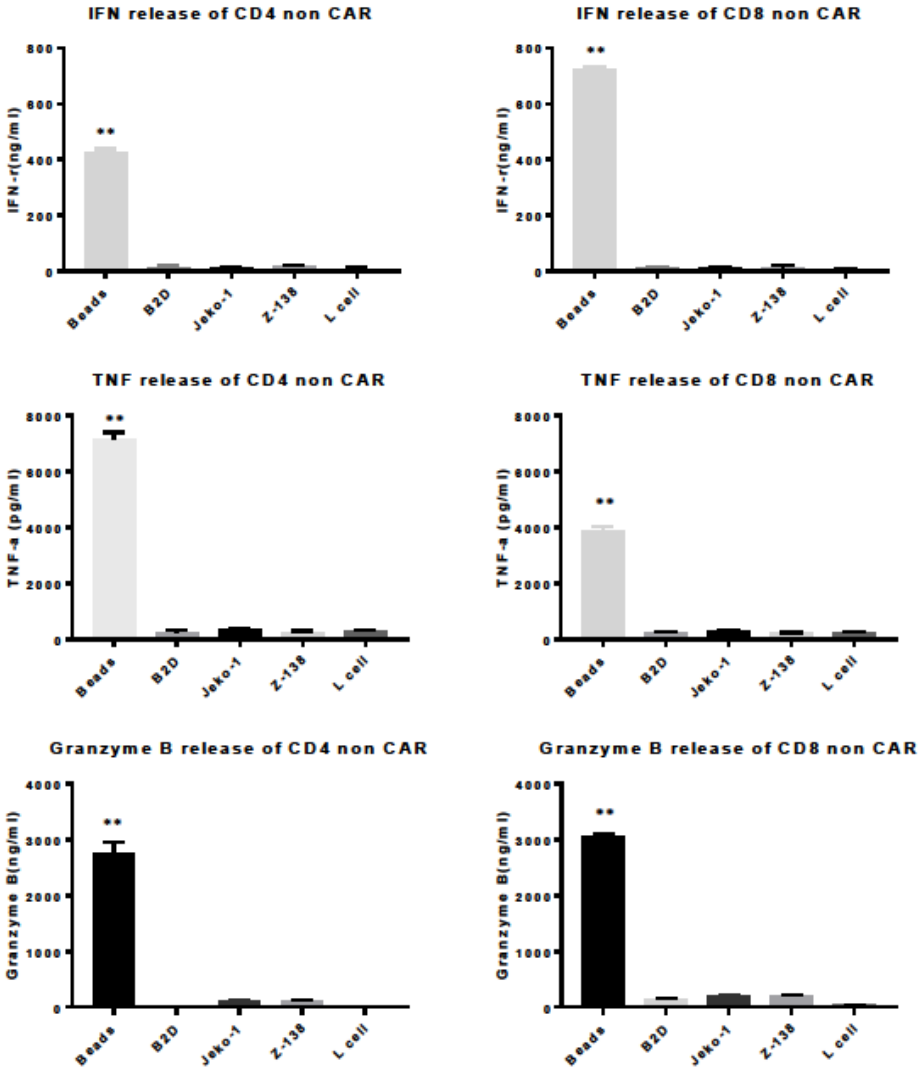

Fig. S1. Cytokine release assay. Either CD4+ or CD8+ T cells were incubated with BAFF-R expressing L cells, mantle cell lymphoma (MCL) lines JeKo-1, Z-138, or as controls, parental L cells (mouse fibroblast) or T-activator CD3/CD28 beads (Allogeneic controls for Fig. 1A). IFN-γ, TNF-α, and granzyme-B were measured by ELISA following incubation with non-transduced T cells from the same donor. Data are

represented as mean ± s.d. of triplicates. The same donor T cells were used as in Fig. 1A. One-way ANOVA and Dunnett's multiple comparisons test: **P<0.0001 vs. L cell control.

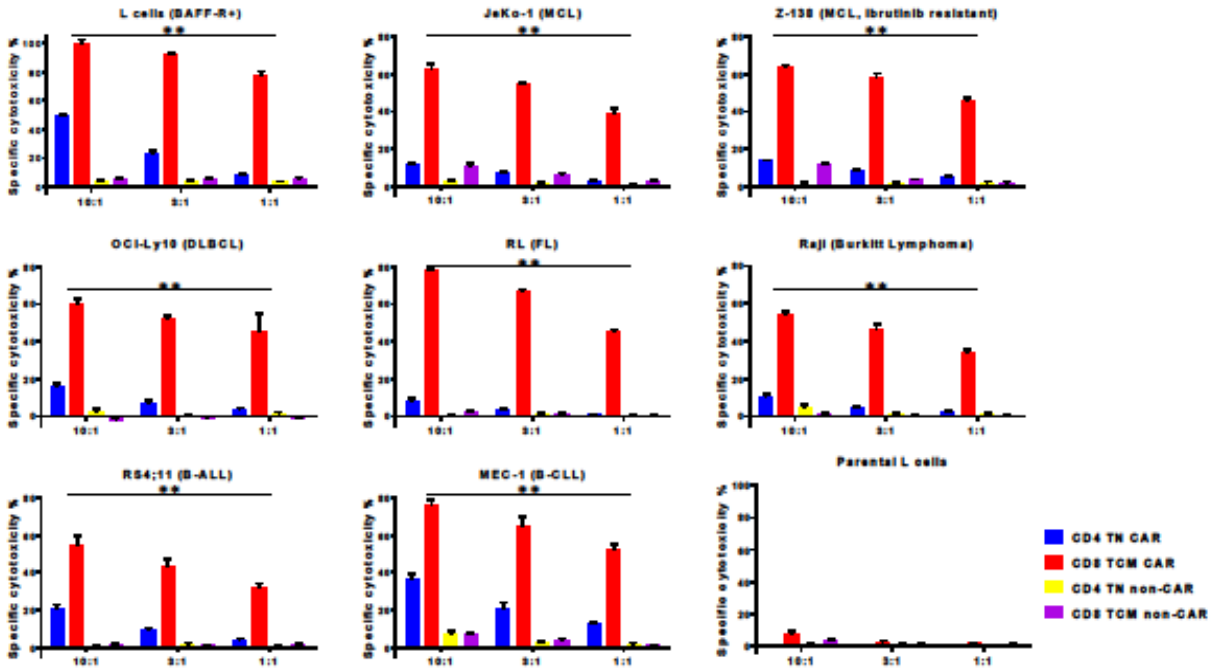

Fig. S2. BAFF-R CAR-T cell *in vitro* CTL assay. Cytotoxic T lymphocyte assay measuring the specific lysis of target cells by chromium-51 release after 4 hours. Additional effector-to-target ratios are shown in addition to Fig. 1B. Various Chromium-51 labeled BAFF-R-positive lymphoma and leukemia cell lines, BAFF-R-positive L cells, or control BAFF-R-negative parental L cells were incubated with either CD4 or CD8 CAR-T cells. Data are represented as mean ± s.d. of triplicates. Two-way ANOVA and Tukey's multiple comparisons test: **P<0.001 vs. corresponding non-CAR control.

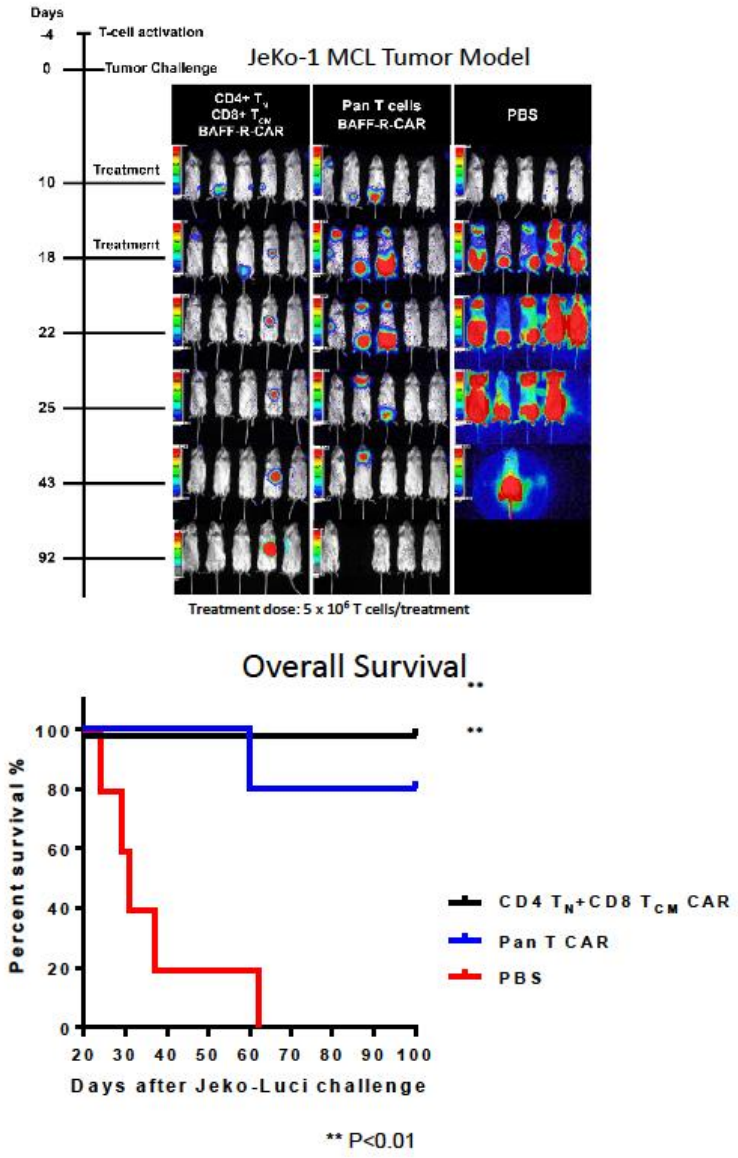

Fig. S3. Preliminary BAFF-R CAR-T cell assessment *in vivo*. Bioluminescence images and overall survival of groups of 5 NSG mice following intravenous (IV) tumor challenge (10^6 cells/mouse) on day 0 with luciferase-expressing human MCL line JeKo-1. Activated BAFF-R CAR-T cells (1:1 CD4 T_N + CD8 T_{CM} or Pan T cells) were infused IV on days 10 and 18 at a dose of 5 x 10^6 cells. Control mice received PBS only. Survival data were analyzed by Kaplan-Meier plots of overall survival at 100 days. Log-rank test: **P<0.01 compared to control.

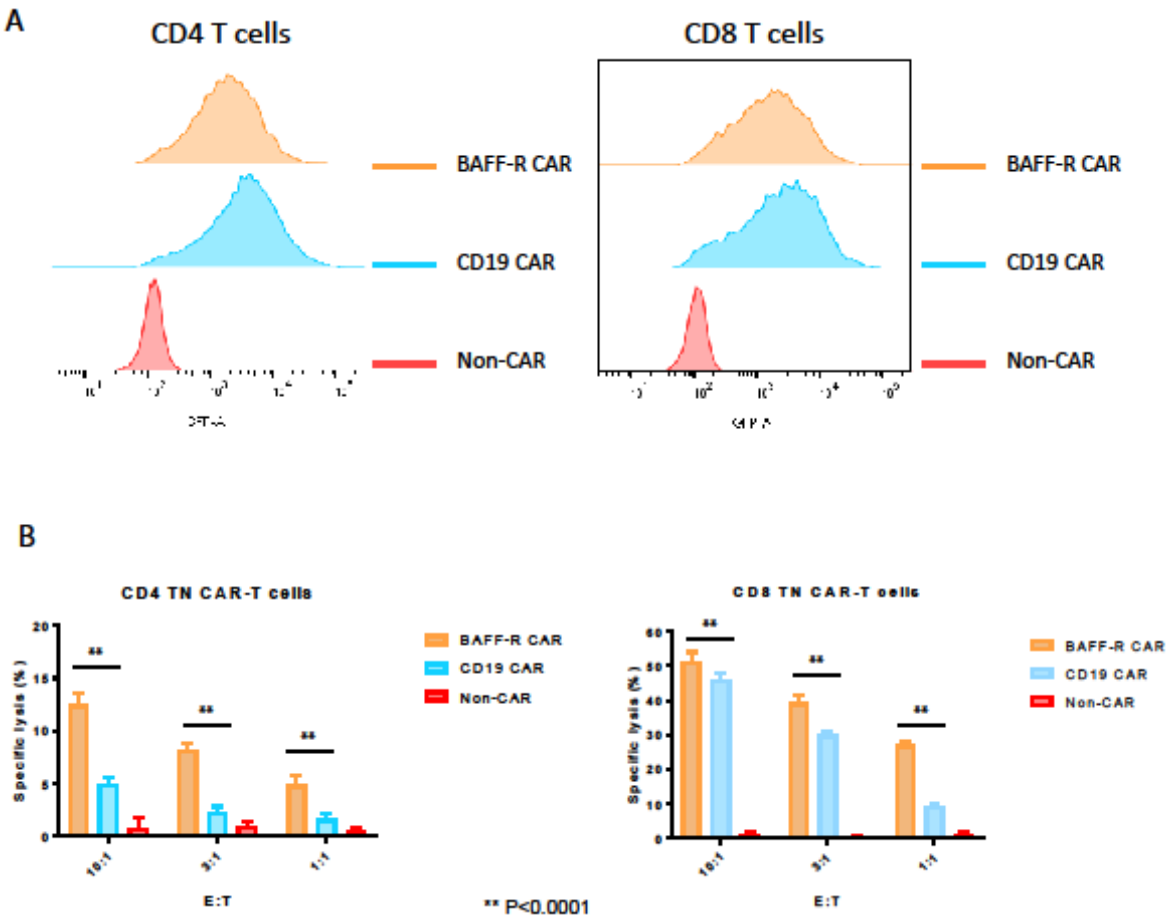

Fig. S4. CAR-T cells validated for CAR expression and CTL activity. Prior to experimental assays, each batch of CD4 and CD8 CAR-T cells were analyzed. **(A)** FACS histograms of CAR-T cells for the expression of GFP associated with CAR expression. **(B)** Calculated specific lysis of Raji cells post co-incubation with either CAR-T cells. BAFF-R or CD19 CAR-T cells from the same donor was incubated with Raji at effector to target ratio (E:T) as shown. Lysis values are represented as mean ± s.d. of triplicates. Non-CAR-transduced T cells from the same donor were used as controls. Data are representative of each batch of CAR-T cells produced. Two-way ANOVA and Tukey's multiple comparisons test: **P<0.001 vs. non-CAR control.

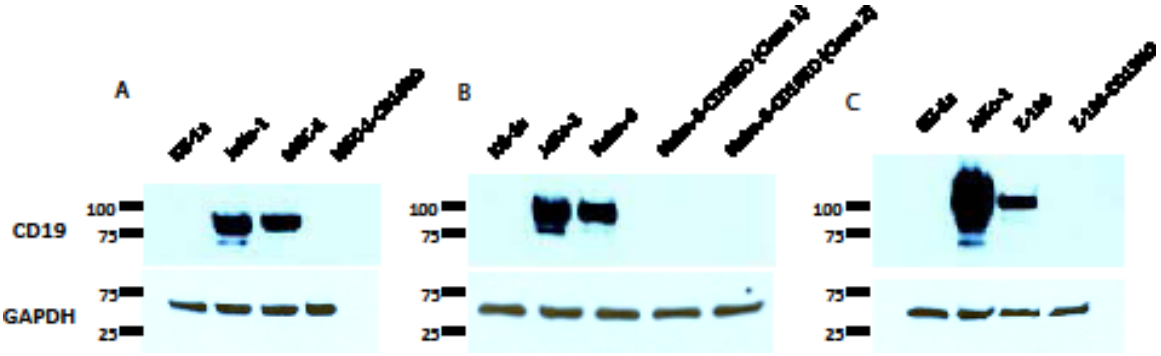

Fig. S5. CD19-KO clone selection. Western blots with anti-CD19 antibody on total cell lysate from parental and CD19-knock-out cell lines as shown: **(A)** MEC-1 (CLL); **(B)** Nalm-6 (ALL); and **(C)** Z-138 (MCL). CD19-knock-out clones were generated by CRISPR/HDR system. KG-1a (acute myeloid leukemia) and JeKo-1 (MCL) were used as cell line controls. Anti-GAPDH antibody was used as a loading control.